



HAL
open science

Impact of freeze-thaw cycles on organic carbon and metals in waters of permafrost peatlands

Dahédrey Payandi-Rolland, Liudmila S Shirokova, Fabian Labonne, Pascale Bénézeth, Oleg S Pokrovsky

► **To cite this version:**

Dahédrey Payandi-Rolland, Liudmila S Shirokova, Fabian Labonne, Pascale Bénézeth, Oleg S Pokrovsky. Impact of freeze-thaw cycles on organic carbon and metals in waters of permafrost peatlands. *Chemosphere*, 2021, 279, pp.130510. 10.1016/j.chemosphere.2021.130510 . hal-03363287

HAL Id: hal-03363287

<https://hal.science/hal-03363287>

Submitted on 3 Oct 2021

HAL is a multi-disciplinary open access archive for the deposit and dissemination of scientific research documents, whether they are published or not. The documents may come from teaching and research institutions in France or abroad, or from public or private research centers.

L'archive ouverte pluridisciplinaire **HAL**, est destinée au dépôt et à la diffusion de documents scientifiques de niveau recherche, publiés ou non, émanant des établissements d'enseignement et de recherche français ou étrangers, des laboratoires publics ou privés.

1
2
3
4
5
6
7
8
9
10
11
12
13
14
15
16
17

Impact of freeze-thaw cycles on organic carbon and metals in waters of permafrost peatlands

DAHÉDREY PAYANDI-ROLLAND^{1*}, LIUDMILA S. SHIROKOVA^{1,2}, FABIAN LABONNE¹, PASCALE BÉNÉZETH¹, OLEG S. POKROVSKY^{1,3}

¹ *Geoscience and Environment Toulouse, UMR 5563 CNRS, University of Toulouse, 14 Avenue Edouard Belin, Toulouse, France*

² *N. Laverov Federal Center for Integrated Arctic Research of the Ural Branch of the Russian Academy of Sciences, Arkhangelsk, Nab Severnoi Dviny 23, Russia*

³ *BIO-GEO-CLIM Laboratory, Tomsk State University, 35 Lenina Pr., Tomsk, Russia*

*corresponding author at: 14 Avenue Edouard Belin, Observatoire Midi-Pyrénées (Laboratoire GET), 31400 Toulouse (France) ; email: dahedrey.payandirolland@hotmail.com (D. Payandi-Rolland)

Key words: ice, moss, lichen, peat, thermokarst lake, river

18 **Abstract**

19 Despite the importance of soil and surface waters freezing in permafrost landscapes,
20 the behaviour of dissolved organic carbon (DOC), nutrients and metals during periodic freeze-
21 thaw cycles (FTC) remains poorly known. The on-going climate warming is likely to increase
22 the frequency of FTC in continental aquatic settings, which could modify the chemical
23 composition of waters. In this study, we conducted 9 repetitive cycles of overnight freezing (-
24 20 °C) and 5 hours thawing (4°C) in the laboratory using representative 0.22 µm-filtered
25 waters from NE European permafrost peatland: leachates of vegetation and soil, and natural
26 surface waters (depression, thermokarst lake and river). Only minor (< 5% - 15%) changes of
27 DOC concentrations, SUVA₂₅₄ and molecular weight were observed in all leachates and the
28 depression water. In contrast, several trace elements (Fe, Al, P, Mn, As, and REE) exhibited
29 sizable variations during FTC (> 10%). The leachates and the depression water were enriched
30 in trace elements, whereas the thermokarst lake and the river demonstrated a decrease in
31 concentration of Fe (-39 and -94 %, respectively), Al (-9 and -85 %), and Mn (-10 and -79 %)
32 during FTC. Overall, the observations demonstrated an increase in aliphatic low molecular
33 weight organic matter (OM), and the precipitation of Fe, Al hydroxides and organo-mineral
34 particles. Therefore, enhanced of frequency of FTC can favour the release of metals and
35 toxicants from acidic OM-rich surface waters and maintain stable OM-metals-colloids in large
36 lakes and rivers, thus regulating aquatic transport of DOC and metals from soils to the Arctic
37 Ocean.

38

39 **1. Introduction**

40 In Arctic regions, strong permafrost thaw occurs mostly where soil temperature
41 fluctuates around 0 °C (Romanovsky et al., 2010) which corresponds to discontinuous and
42 sporadic permafrost zones. This is especially important in Arctic wetlands such as permafrost
43 peatlands which contain a huge amount of organic carbon (OC) (Hugelius et al., 2014; Schuur
44 et al., 2015). The dissolved OC (DOC) is the main form of terrestrial C exported from soil
45 solutions to rivers and lakes in the wetlands (Chapin et al., 2006; Cole et al., 2007). The
46 transformation of DOC in surface waters involves photo- and bio-degradation which is
47 controlled by light intensity (Selvam et al., 2019), temperature (Boddy et al., 2008), origin of
48 OC and microbial diversity (Young et al., 2005). Transition periods (*i.e.* early spring and late
49 autumn) appeared to be essential times for the export (Manasypov et al., 2015; Pokrovsky et
50 al., 2020) and biodegradation (Payandi-Rolland et al., 2020b) of DOC in rivers and lakes of
51 Arctic wetlands when the majority of DOC originates from leaching of supra-permafrost-soil
52 and vegetation (Ma et al., 2019; Vonk et al., 2015). These periods are dominated by recurrent
53 freeze-thaw cycles (FTC, Henry, 2008). Furthermore, full freezing of thermokarst lake basins
54 in western Siberia was reported to lead to massive coagulation of organo-ferric colloids
55 producing macroscopic, organic- and Fe-rich amorphous particles capable of precipitating to
56 the lake bottom (Manasypov et al., 2015).

57 Since the 1970s, a lot of attention is given to the impact of freezing and thawing on soil
58 properties (DeLuca et al., 1992; Kim et al., 2017; Larsen et al., 2002; Ren and Vanapalli, 2020;
59 Schimel and Clein, 1996; Xiao et al., 2019). In contrast, studies on the influence of freezing and
60 thawing on dissolved solutes of continental waters are only at their beginning (Chen et al.,
61 2016; Hentschel et al., 2008; Pokrovsky et al., 2018; Savenko et al., 2020; Spencer et al., 2007).
62 Most of them focused on surface water with near circum-neutral pH such as rivers (Chen et

63 al., 2016; Savenko et al., 2020) and ponds (Pokrovsky et al., 2018). The main impact noticed
64 by those studies is the decrease of aromaticity in waters due to FTC (Chen et al., 2016) and
65 the generation of low molecular weight (LMW) organic components (Pokrovsky et al., 2018).
66 The impact of freezing on dissolved organic matter (DOM) in high latitudes is still poorly
67 known. In this study, we conducted freeze-thaw experiments aimed to characterize the
68 impact of FTC on DOC, major and trace elements in waters of one of the largest permafrost
69 peatlands of Europe, the Bolshezemelskaya Tundra (BZT). For this, we used DOM originated
70 from vegetation, soil (peat) and natural water bodies of this peatland. Based on a few available
71 studies dealing with FTC of surface waters (Fellman et al., 2008; Pokrovsky et al., 2018; Xue et
72 al., 2015), we hypothesized that: 1) DOC and trace metals (TM) present in the form of organic
73 and organo-mineral colloids could coagulate under freezing which could favour the transport
74 of mineral under more stable forms (colloids) through lakes and rivers to the Arctic Ocean; 2)
75 OC originated from fresh plant biomass (i.e. leachates not subjected to previous freezing)
76 would be more sensitive to FTC compared to natural waters, as fresh DOC is known to be
77 composed of more labile components, and 3) the FTC could have a more pronounced effect
78 on the degradation of OC from the permafrost compared with active layer OC since the latter
79 has undergone previous seasonal freezing cycles. Overall, we aimed at providing an empirical
80 assessment on the degree of DOC and inorganic solutes concentrations change after repeating
81 freezing and thawing of representative surface waters from permafrost peatlands.

82

83 **2. Materials and methods**

84 *2.1. Substrates origins and use*

85 The DOM used in this study originated from: *i*) natural surface waters of a permafrost
86 peatland, *ii*) aqueous leachates of ground vegetation and *iii*) aqueous leachates of peat soil.

87 The sampling sites are located in the NE European permafrost peatlands (BZT) within the
88 discontinuous permafrost zone. Natural waters were collected from a small depression, a
89 thermokarst lake and the Pechora River (Supplementary **Table S1**). Waters were filtered on-
90 site through a 0.45 μm sterile filtration unit and re-filtered in the laboratory through a 0.22
91 μm Nalgene sterile filter before freezing.

92 The soil and ground vegetation for leachates were collected at the shore of the
93 thermokarst lake (**Table S1 and Figure S1**). The peat core was sampled using a Russian peat
94 corer (see details of sampling and handling in [Morgalev et al., 2017](#)). The soils included two
95 subsamples of peat, one collected in the active (unfrozen) layer (20-30 cm below the surface)
96 and the second one in the permafrost zone (> 30-40 cm). Both subsamples represent
97 oligotrophic peat composed of *Sphagnum angustifolium*, cotton-grass *Eriophorum*,
98 *Scheuchzeria palustris*, bog-sedge *Carex limosa*, lichens, dwarf shrubs and some amount of
99 wood debris (pine) and green mosses ([Payandi-Rolland et al., 2020b](#)). Ground vegetation
100 contained mosses (*Sphagnum fuscum* and *Sphagnum angustifolium*) and lichens (*Cladonia*
101 genus), which colonize hollows and mounds of the palsa and are reported to be widely spread
102 species in the tundra ([Malmer et al., 2005](#)). Aqueous leachates were prepared by reacting 10
103 g of organic substrate (10 g_{wet} for frozen peat and 10 g_{dry} for vegetation) with 1 L of sterile
104 MilliQ water under constant agitation (70 rpm) at 25 ± 2 °C in the dark and aerobic conditions
105 ([Payandi-Rolland et al., 2020b](#); [Shirokova et al., 2017a, 2017b](#)). After 3 days of reactions, the
106 suspension was centrifuged at 4500 g for 5 minutes and then sterile filtered (< 0.22 μm) using
107 500 mL Nalgene units and a manual vacuum pump.

108

109 2.2. *Incubation, freeze-thaw cycles and sampling*

110 A 150 mL aliquot of each leachate and natural waters were placed in pre-cleaned
111 (rinsed 3 times with HCl (1 M) and MQ water and then autoclaved at 121 °C for 20 min) 200
112 mL polypropylene Nalgene bottles. Experiments with each substrate were performed in
113 duplicate. A cycle of freeze-thaw (adapted from [Pokrovsky et al., 2018](#)) started from placing
114 water-filled Nalgene bottles in the freezer (-20 °C) overnight. After the total freeze of the
115 liquid, bottles were transferred into the refrigerator compartment (at 4 °C) and kept there for
116 5 hours until the ice melted completely. These temperatures can be observed at the
117 permafrost peatlands during the year in winter ([Lim et al., 2021](#)), early spring and late autumn
118 (“[Climate & Weather Averages in Naryan-Mar, Russia,](#)” 2015; [Serikova et al., 2019](#)) and are
119 consistent with the range used in previous works ([Chen et al., 2016](#); [Pokrovsky et al., 2018](#);
120 [Spencer et al., 2007](#); [Xue et al., 2015](#)). All filtrates have undergone 9 FTC, which corresponds
121 to the average number of annual freeze-thaw cycles observed in high-latitude boreal and
122 Arctic regions ([Henry, 2008](#); [Pokrovsky et al., 2018](#)).

123 After total ice melt in each cycle, we sampled 15 mL of a homogeneous aliquot from
124 the bottle. Before and during the sampling, bottles were vigorously stirred with a magnetic
125 stir bar to provide homogeneous suspension and avoid selective removal of either dissolved
126 or particulate phase. A non-filtered subsample was used to measure pH (uncertainty of ± 0.01
127 pH units) and specific conductivity ($\pm 0.1 \mu\text{S}\cdot\text{cm}^{-1}$). The rest of the 15 mL was filtered through
128 a 0.22 μm filter (sterilizing filtration, Minisart® syringe filter). In the filtrates, the DOC was
129 measured with Shimadzu TOC-VSCN with an uncertainty of 2%. The UV-absorbance of water
130 samples was measured using a 10 mm quartz cuvette on a CARY-50 UV-vis
131 spectrophotometer, between 200 and 700 nm. The UV and visible spectra allowed assessment
132 of (i) the molecular weight (MW) of DOC *via* the Weight-Average Molecular Weight index

133 (WAMW, using the absorbance at 280 nm, [Chin et al., 1994](#)), (ii) the humification index using
134 the ratio of absorbance at 250 and 400 nm (the E2:E4 ratio, [Park et al., 1999](#)) and (iii) the
135 aromaticity of incubated water *via* specific UV absorbance (SUVA₂₅₄) ([Abbt-Braun and
136 Frimmel, 1999](#)). Major cations (Na, Ca, K and Mg), Si, P and trace elements (TE) were measured
137 with a quadrupole ICP-MS (Agilent 7500 ce) using In+Re as an internal standard. The
138 international geo-standard SLRS-5 (Riverine Water Reference Material for Trace Metals) was
139 used to check the validity and reproducibility of analyses.

140

141 2.3. Treatment of experimental results

142 Statistical treatment involved the least square method for regression and the Pearson
143 correlation. All statistical analysis has been accomplished under R-software (version 3.6.2).
144 Boxplot analyses were used to detect outliers. Boxplot values combine the median (Q₂), the
145 first quartile (Q₁), the third quartile (Q₃), and the interquartile range (IQR) which is defined as
146 the difference between Q₃ and Q₁. Outliers are defined as values located outside the first (D₁)
147 and the last (D₉) decile, as “D₁ = Q₁ - 1.5*IQR” and “D₉ = Q₃ + 1.5*IQR” ([Tukey, 1977](#)). Linear
148 regression analyses have been performed using the function “lm” of the package “stats”. The
149 percentage of component gain or loss during FTC (ΔFTC_{0-9} , %) was calculated as a difference
150 in concentration between the final and initial concentration of a component, normalized to
151 its initial concentration. Trace element complexation with OM and saturation indices of the
152 solution with respect to common solid phases were calculated using the Visual MINTEQ
153 (vMINTEQ) software, following the model specifications for organic-rich waters of permafrost
154 peatlands describe elsewhere ([Pokrovsky et al., 2016, 2018](#)). A dataset combining the
155 measured parameters can be found in [Payandi-Rolland et al. \(2020a\)](#).

156

3. Results and Discussion

3.1 Chemical composition of aquatic substrates

The dissolved (<0.22 μm) concentrations of DOC, major and trace elements of substrates used in this study are reported in **Table 1**. The water samples ranged from acidic (peat and vegetation leachates) to circum-neutral (depression, thermokarst lake, and Pechora River). The DOC of the thermokarst lake and the river was < 10 mg L^{-1} , which is 2 times lower than the leachates of peat and moss, 5 times lower than the lichen leachate, and 10 times lower than the water of depression. Such a wide range is comparable to the one reported for the hydrological continuum (depression \rightarrow lake \rightarrow stream \rightarrow river) of this region (Shirokova et al., 2019). In all substrates, the DIC was below 1.5 mg L^{-1} except for the Pechora River (10.4 mg L^{-1}). The SUVA_{254} ranged from low (< 2 $\text{L mgC}^{-1} \text{m}^{-1}$) for the lichen leachate and the depression to near 4 $\text{L mgC}^{-1} \text{m}^{-1}$ in other natural waters, and finally to values > 5 $\text{L mgC}^{-1} \text{m}^{-1}$ for leachates of soils and moss. The WAMW of all substrates was lower than 3 kDa and ranged from ≤ 1 kDa in lichen leachate and the depression to near 2-2.5 kDa in other natural waters and in soil and moss leachates. Considering that the MW of fulvic acids (Fa) is approximately 600 to 1000 Da and that the humic acid (Ha) MW is between 1500 and 5000 Da, (Garcia-Mina, 2006; Malcolm, 1990), 3 groups of samples could be distinguished in terms of DOM character: i) the humic OM group with a strong influence of Ha (*i.e.* leachates of soils and moss), ii) the “mixed” OM group with both influence of humic and fulvic acids (HFa) (*i.e.* the thermokarst lake and the Pechora River) and iii) the Fa OM group (*i.e.* lichen leachate and the water from the depression).

The leachate of lichen and the water from depression exhibited the highest DOC concentration (respectively 53 and 107 mg L^{-1}), and lowest WAMW (758 ± 1 and 1121 ± 7 Da) and SUVA_{254} (0.7 and 1.6 $\text{L mgC}^{-1} \text{m}^{-1}$). This indicates that the DOC of these samples is mostly

181 composed of simple OC molecules with the dominance of aliphatic components ([Ågren et al.,](#)
182 [2008](#); [Tranvik and Jørgensen, 1995](#); [Weishaar et al., 2003](#)). Conversely, other waters exhibited
183 lower DOC concentrations with a high proportion of aromatic compounds (**Table 1**).
184 Considering the observed large difference in concentration of DOC, aromatic/aliphatic
185 composition and the molecular weight of waters, it is anticipated that the effect of FTC could
186 be primarily linked to these parameters. The concentrations of major and trace elements
187 strongly varied among samples with general dominance of alkali and alkaline earth metals
188 such as Ca, Na, Mg and K (**Table 1**). The highest concentrations of metals (Fe, Al, Mn) were
189 observed in the moss leachate and depression waters (**Table 1**). Other trace elements
190 exhibited concentrations lower than 2 µg L⁻¹.

191

192 *3.2 Visual impact of the freezing process on DOM and removal of outliers*

193 After full freezing of experimental reactors, ice was transparent at the borders and
194 brown in the centre of bottles, similar to other FTC experiments (e.g., [Pokrovsky et al., 2018](#)).
195 The concentration of brownish components (chromophoric components) in the centre of the
196 bottle reflects the progressive freezing of water from bottle edges to the centre with a relative
197 accumulation of DOM in the remaining liquid ([Petzold et al., 2013](#); [Shafique et al., 2012](#); [Xue](#)
198 [et al., 2015](#); [Zaritzky, 2006](#)). Further, it was shown that a high concentration of DOM and low
199 freezing temperatures diminish the proportion of DOM incorporated in the ice phase ([Elliott](#)
200 [and Henry, 2009](#); [Hentschel et al., 2008](#); [Shafique et al., 2012](#); [Xue et al., 2015](#)). The high
201 concentration of DOC in leachates of soils and moss (around 20 mg L⁻¹), in the leachate of
202 lichen (53 mg L⁻¹) and in the water from the depression (106 mg L⁻¹) associated to the -20 °C
203 temperature used in this study promotes the segregation of DOM in the remaining fluid
204 located at the centre of the bottle during the freezing process. Such a formation of brown

205 coagulates in the ice was interpreted as a change in particles density and diameter that occurs
206 during the freezing (Fellman et al., 2008; Giesy and Briese, 1978), and presumably, leads to
207 the formation of organo-metal aggregates rich in Fe and Al hydroxides (see **section 3.5**). It is
208 worth noting that after the total thaw of waters, no visual aggregations of OM (brownish area)
209 can be distinguished in liquid. Furthermore, conversely to the FTC experiments on an organic-
210 rich bog and fen waters (Pokrovsky et al., 2018), no brown/yellow precipitates have been
211 observed at the bottom of the containers. From this observation, we hypothesized apparent
212 reversibility of organic colloids and particles aggregation-dissolution during FTC of studied
213 waters.

214 Preliminary analysis of the DOC concentration evolution during the FTC demonstrated
215 some clear outliers. A boxplot repartition on data revealed that some of the data points can
216 be statistically considered as outliers (see description of outliers given in **section 2.3; Figure 1**
217 and **Table S2**). These outliers are believed to be sampling artefacts. Some samples
218 demonstrated an increase in certain elements concentration during FTC, which is
219 counterintuitive given that all samples were 0.22 μm filtered prior to the incubation and also
220 0.22 μm filtered at each sampling. Furthermore, these increases were non-systematic and
221 non-reproducible among replicates. We hypothesize that FTC can generate aggregates of DOC
222 and metal hydroxides (see **section 3.5**) thus producing some “islands” of solute-rich and
223 solute-poor fluids. During the sampling procedure, even under continuous stirring, one can
224 randomly collect some aggregate-enriched aliquots. Because *i)* each sampling are
225 independent and *ii)* the presence of such aggregates, revealed by abnormal DOC
226 concentrations, can biased other measured parameters (absorbance and trace elements
227 concentrations), we have removed the outliers (about 7% of all collected data, see **Table S2**).

228 In the rest of this study, results and discussions will only deal with the new data set (i.e.
229 without outliers).

230 3.3. Quantification of freeze-thaw cycles impact on DOC concentration and quality

231 The evolution of DOC concentration during FTC (**Figure 1**) exhibited variable trends
232 among samples. The DOC concentration slightly increased between the initial stage (prior to
233 the first freezing, *i.e.* FTC0) and after the last freezing (FTC9) in the active layer leachate ($5 \pm$
234 2%), the thermokarst lake (8%) and the Pechora River ($14 \pm 4\%$) (**Figure 2** and **Table S3**). The
235 variations of DOC in other samples were lower than 5%. However, only the increase of
236 thermokarst lake DOC with FTC was superior to 5% and significant ($p_value < 0.05$; **Figure 2**
237 and **Table S4**). Former studies demonstrated generally decreasing DOC concentration in the
238 course of FTC with a range of DOC loss from 7 to 25% (Fellman et al., 2008; Pokrovsky et al.,
239 2018). Fellman et al. (2008) demonstrated that the initial concentration of DOC strongly
240 influenced the removal efficiency, with a loss of 7% when the concentration was $< 5 \text{ mg L}^{-1}$
241 and a 20% loss at higher initial DOC concentrations. In the present study, all initial DOC
242 concentrations were superior to 7 mg L^{-1} and waters with the lowest initial concentration
243 (from 7 to 10 mg L^{-1} , **Table 1**) exhibited an increase in DOC (*i.e.* the Pechora River and the
244 thermokarst lake, **Figure 2** and **Table S3****Erreur ! Source du renvoi introuvable.**). Therefore,
245 the initial concentration of DOC does not appear to control the DOC removal efficiency in our
246 study. Overall, low variations of DOC ($< 5\%$, at the exception of the thermokarst lake and the
247 Pechora River water) highlight the high stability of DOC when subjected to FTC. This
248 observation is in agreement with the study by Xue et al. (2015) showing that DOC
249 concentrations of lotic waters (which froze on 1 m thick during 3 to 5 months per year in the
250 northern China) were highly stable (from 0.68% increase to 4.3% decrease) through FTC.

251 The SUVA₂₅₄ values presented in this work do not take into account the iron corrections
252 suggested by [Poulin et al. \(2014\)](#) because the differences between the uncorrected and
253 corrected SUVA₂₅₄ values were below 5% for all incubated substrates at the exception of the
254 depression (maximum 5.9%), see **Table S5**. The SUVA₂₅₄ and WAMW values decreased (from -
255 6.5% to $-(17.0 \pm 1)\%$, and from -5.6 % to $-(14.1 \pm 1)\%$, respectively) between FTC0 to FTC9 in
256 the thermokarst lake and the Pechora River, whereas in other samples, the variations were
257 below 5% (**Figure 2**, **Figure S2** and **Table S3**). Given that the waters were sterile filtered (< 0.22
258 μm) before the experiments, the observed decrease of SUVA₂₅₄ and WAMW can be only
259 abiotically driven. This suggests that the FTC can provide an increase in non-aromatic low
260 molecular weight components in waters from moss leachates, thermokarst lake and Pechora
261 River. At the same time, both variations of SUVA₂₅₄ and WAMW in waters of thermokarst lakes
262 and Pechora River were not significantly correlated to the number of FTC (**Table S4**).

263 The evolution of E2:E4 ratio between the 0 and 9th cycle of freezing was null to positive
264 in all leachates ($< 5\%$ increase), clearly positive in the depression (an increase of 8.5%), and
265 negative in the thermokarst lake and the Pechora River (-5.2% and $-(5.6 \pm 2)\%$, respectively,
266 **Figure 2** and **Table S3**). In the present study, the relative removal of humic-like aromatic
267 components in waters from the HFa group (see **section 3.1**, *i.e.* the thermokarst lake and the
268 Pechora River) is corroborated by a decrease of SUVA₂₅₄ and WAMW values through FTC in
269 these samples (**Figure 2** and **Figure S3**). Unlike well-known biotically-driven degradation of
270 humic-like aromatic components in streams and rivers waters demonstrated by the decrease
271 of E2:E4 ratio ([Hutchins et al., 2017](#)), in this study the decrease of this ratio is imputed to FTC
272 (abiotic phenomenon) which appear to be also capable of selective removal of humic-like
273 aromatic compounds in the lake and river water. In contrast, in leachates and depression

274 waters, while the E2:E4 ratio slightly (< 10 %) increased with FTC, no evidence of selective
275 removal of LMW components have been detected (the WAMW variations were < 5%).

276

277 3.4. Trace element behaviour during FTC

278 A clear decrease of Fe concentration during FTC in thermokarst lake and the Pechora
279 River (-39.0% and -94.4%; respectively; **Figure 3, Figure S4** and **Table S3**) suggests the removal
280 of this element in the form of secondary phases. The saturation index (SI) calculated *via* the
281 vMINTEQ software indicates that Fe can precipitate in the form of akaganeite
282 ($\text{FeO}_{0.83}(\text{OH})_{1.17}\text{Cl}_{0.17}$, SI: 1.8 to 2.1), goethite ($\text{Fe}(\text{OH})_3$, SI: 0.7 to 1.0) and lepidocrocite
283 ($\text{Fe}^{3+}\text{O}(\text{OH})$, SI: 0.6 to 0.9) in all surface waters. In the case of thermokarst lake and the Pechora
284 River, a significant ($p < 0.05$) increase in (C_{org}/Fe) molar ratio in the course of FTC was observed,
285 which suggested a progressive depletion of Fe relative to C_{org} in the colloidal fraction (**Figure**
286 **4A and C**, and **Table S4**).

287 Aluminium concentration decreased during FTC of moss leachate (-33.4%),
288 thermokarst lake (-9.4%) and Pechora River ($-85.1 \pm 7\%$) samples (**Figure 4, Figure S5** and **Table**
289 **S3**). The SI calculation did not indicate any supersaturation concerning Al oxyhydroxides.
290 However, the formation of organo-mineral (Fe, Al) coagulates *via* coprecipitation of Fe and Al
291 oxyhydroxides is likely given the sizable correlation ($p < 0.05$) between aqueous
292 concentrations of Fe and Al in the course of the FTC sequence (**Figure S6**) in all waters (with
293 an exception of moss leachate). In the case of the Pechora River, a significant ($p < 0.05$)
294 evolution of the molar ratio (C_{org}/Al)_{molar} with the number of FTC (**Figure 4B** and **Table S4**)
295 suggests the formation of mixed Fe-Al-OM sub-colloidal particles as it is reported in surface
296 waters of permafrost peatlands (Pokrovsky et al., 2016). Other trivalent hydrolyses such as
297 Y and Ga punctually correlated with DOC and Fe during FTC (**Figure S7** and **Table S6**). Light REE

298 (LREE: La, Ce and Pr) correlated with Fe in the leachate of the active layer and the permafrost,
299 and in waters of the depression and the Pechora River, whereas heavy REE (HREE: Nd, Dy, Yb)
300 significantly correlated with Fe in the Pechora River (**Table S6**).

301 Phosphate is known to be controlled by dissolved humic substances ([Fellman et al.,](#)
302 [2008](#); [Francko, 1986](#); [Jones et al., 1988](#)) especially in wetlands where the high concentration
303 of DOM and iron facilitates the complexation of DOC and PO₄ ([Dillon and Molot, 1997](#)).
304 However, this was not observed in this study, because there was no correlation between the
305 concentration of PO₄ and DOC, and the molar ratio between organic carbon and phosphate
306 did not systematically vary during the FTC in all samples (**Table S4**). Chromium, vanadium and
307 silicon concentrations decreased in waters of thermokarst lakes and Pechora River (**Figure S8**
308 and **Table S3**), whereas most of the divalent macro- and micro-nutrients (Co and Ni) exhibited
309 a slight increase in concentration through FTC in all waters (**Figure S8** and **Table S3**).

310 Manganese concentration clearly decreased in thermokarst lake and the Pechora River
311 (respectively -10.4% and -(79.4 ±1) %) but remained stable or increased in other waters (**Figure**
312 **3, Figure S9** and **Table S3**). The decrease of Mn concentration and the correlation between
313 the molar ratio (C_{org}/Mn)_{molar} and FTC number could indicate a formation of Mn (hydr)oxide
314 particles or Mn coprecipitation with organo-ferric compounds in the water of the Pechora
315 River.

316 Among tetravalent hydrolysates, Ti and Zr demonstrated an increase in the Pechora
317 River and a decrease in other waters (**Figure S7**). Titanium concentration significantly
318 correlated with Fe in all waters (except the moss leachate). Zirconium correlated with Fe in
319 the leachate of the active layer, permafrost and in the depression. Hafnium and Th correlated
320 with Fe only in water of the depression (**Table S6**). These types of correlation between Fe and
321 insoluble tetravalent hydrolysates have been observed previously in ultrafiltration

322 experiments on boreal forest (Illina et al., 2016) and permafrost surface waters (Pokrovsky et
323 al., 2016) and indicate the dominance of organo-ferric high molecular weight colloids in TE⁴⁺
324 speciation.

325 Lead concentration increased in the course of FTC in all leachates and decreased in
326 natural waters (Figure S7 and Table S3). Arsenic (As) decreased only in the Pechora River
327 water (Figure 3, Figure S10 and Table S3). In riparian wetlands, the presence of As hotspots
328 due to As association with Fe or OM was reported (Guénet et al., 2016). In the present study,
329 linear regressions on As and DOC concentrations were non-significant ($p > 0.05$) in all samples
330 (Table S6). In contrast, there was a strong linear regression ($p < 0.03$) between As and Fe
331 concentrations for all studied samples, except the thermokarst lake (Figure S11 and Table S6).
332 It appears then, that the As is bound to the Fe and not to the OM of either vegetations and
333 soils leachates or natural waters. In addition to its control by DOM, As in natural waters can
334 be adsorbed to Fe-oxyhydroxides, such as nano-lepidocrocite (Guénet et al., 2016). Both the
335 correlation between As and Fe concentrations and the supersaturation of solutions with
336 respect to Fe-oxyhydroxides and lepidocrocite secondary phases (section 3.4) observed in the
337 present study support this hypothesis.

338

339 3.5. Possible mechanisms of DOC and metal transformation during FTC.

340 Two colloidal pools are responsible for TE speciation in boreal aquatic environments:
341 i) small organic-rich colloids and LMW DOM, and ii) high molecular weight Fe-rich colloids
342 (Baalousha et al., 2006; Krachler et al., 2012; Stolpe et al., 2013). The LMW colloids dominate
343 metal speciation in acidic thaw pond water and are highly stable during FTC. In contrast, high
344 molecular weights colloids dominated mainly in neutral waters of the permafrost area and are
345 subjected to strong removal during freezing (Pokrovsky et al., 2018). In our study, the MW of

346 Ha and HFa group can be indicative of LMW colloids (generally ranging between 1 to 50 kDa),
347 while the Fa group (lichen leachate and depression waters) exhibited essentially dissolved
348 fraction (LMW_{<1 kDa}). The LMW_{1-50 kDa} colloids are likely to dominate the metals speciation in
349 the thermokarst lake and the Pechora River water. The stronger impact of FTC on the Pechora
350 River and the thermokarst lake water suggests that mixed HFa OM of large terminal water
351 bodies is most vulnerable to the freeze-thaw process. This observation can be attributed to
352 the two binding patterns of metals and OM. These patterns depend on the maximum metal
353 binding capacity of *i*) humic-like component which is reached at neutral to alkaline pH (7 to 9)
354 due to maximal ionization of carboxylate and phenolic acids; and *ii*) fulvic-like component
355 reached at acidic pH (5 to 6) when the majority of carboxylate moieties are dissociated (Garcia-
356 Mina, 2006). Therefore, in contrast to more acidic plant and peat leachates, in the Pechora
357 River, both the presence of humic acids (in HFa) and the neutral pH (7) and in thermokarst
358 lake, the presence of fulvic acids (in HFa) and slightly acidic conditions (pH = 6.3), promote the
359 aggregation of colloidal Fe *via* DOM - metal binding. Considering, based on our experimental
360 observations, a relatively stable concentration of DOC, a decrease of SUVA₂₅₄, WAMW, Fe
361 concentrations, and an increase in C_{org}/Fe ratio in the course of FTC, we suggest preferential
362 degradation of humic-like components in waters from thermokarst lake and Pechora River
363 and formation of aliphatic LMW_{1-50kDa} colloids. On the contrary, no evidence on the formation
364 of organic and organo-ferric colloids in other waters during FTC has been detected in our
365 study.

366

367 *3.6. Possible role of FTC in natural environments*

368 Progressive accumulation of DOM and related elements in the remaining fluid due to
369 full freezing of the water column is observed in shallow confined natural water bodies such as

370 thermokarst lakes and ponds of permafrost peatlands (Manasypov et al., 2015). In the present
371 study, the effect of freezing on concentrations of most dissolved components did not generally
372 exceed 10% and was limited to simple physicochemical reactions given that all samples were
373 sterile-filtered before the first freezing. In contrast, in a non-sterile FTC experiment that used
374 various soils from marsh and wet grasslands, a strong DOC production (100 to 300 mg L⁻¹)
375 compared to samples not subjected to FTC was reported (Yu et al., 2011). This increase was
376 believed to be the consequence of microbial cells lysis, physical disruption of soils aggregates,
377 and roots turnover (Bochove et al., 2000; DeLuca et al., 1992; Ivarson and Sowden, 1970;
378 Tierney et al., 2001). In natural permafrost aquatic and soil environments, microbial
379 communities are highly resistant to FTC (Lipson and Monson, 1998; Stres et al., 2010). This
380 suggests that both the capacity of micro-organisms to quickly recover and efficiently
381 biodegrade OM, together with the abiotic transformation of DOC during and after repetitive
382 freezing can become a sizable source of LMW DOC, as also reported in previous studies
383 (Pokrovsky et al., 2018). Further, whereas the freezing process can impact the DOM
384 concentration, the thawing duration (hours or days) has little effect on the DOC aromaticity
385 of leachates (Hentschel et al., 2008; Vestgarden and Austnes, 2009). This implies that the rapid
386 thawing of ice in nature could lead to the production of more easily biodegradable OM
387 components.

388 The results of the present study demonstrated rather minor (i.e., ≤ 10%) effects of
389 freeze-thaw cycles on DOC quantity and quality in various leachates of soils and vegetation
390 which indicates strong stability of DOM in typical surface waters of boreal peatlands (except
391 large river). As such, the FTC may be of sub-ordinary importance on DOM transformation in
392 surface waters of permafrost peatlands relative to other biotic and abiotic factors such as
393 heterotrophic degradation and photolysis (Payandi-Rolland et al., 2020b; L. S. Shirokova et al.,

394 [2019](#)). In contrast, the “mineral” part of organo-mineral colloids present in natural waters was
395 subjected to removal from solution due to freezing as indicated by an increase in C_{org}/Fe and
396 C_{org}/Al molar ratios in the course of FTC of river and lake water. In this regard, the impact of
397 FTC on trace metal can be competitive to bio- and photo-transformation of trace metal
398 colloids ([Oleinikova et al., 2018, 2017](#)). Therefore, the first hypothesis of this study was
399 confirmed only for the large river, where both Fe and Al were removed preferentially to DOC.
400 For a thermokarst lake, this hypothesis was only partially confirmed (solely Fe removal). Such
401 a removal of Fe, Al and other metal were not observed in vegetation and soil leachates and in
402 the depression water, thus confirming a subsidiary role of freezing on DOM and metal fate
403 in surface waters of permafrost peatlands. This dismisses the second hypothesis of this study
404 on the highest sensitivity of fresh leachates to freezing: regardless of the origin of vegetation
405 leachates (moss and lichen), the change in concentration of DOC and metals during FTC was
406 inferior to that of river and lake waters. In contrast, large water bodies such as the Pechora
407 River or a thermokarst lake meet the ideal conditions for stabilization of OM-mineral colloids.
408 In these settings, the FTC can facilitate aquatic transport of C, nutrients and metals from
409 peatlands surface waters to the Arctic Ocean. However, because the full freezing of large
410 surface water bodies is unlikely compared to small depressions and soil porewaters, the
411 overall impact of FTC on DOC and metal transformations in permafrost peatlands is expected
412 to be low. As such, unlike the bio- and photo-degradation of permafrost DOM in Arctic waters
413 ([Cory et al., 2014; Vonk et al., 2015](#)), which has to be considered in models of the future arctic
414 C balance ([McGuire et al., 2018](#)), the freeze-thaw cycles are likely to be of secondary
415 importance for C transformation in Arctic continental waters.
416

417 **Conclusions**

418 This study demonstrated that the pH and OM composition (aromaticity, molecular
419 weight, proportion of humic and fulvic components) are the main factor controlling the DOC
420 (< 0.22 μm) removal from surface waters of permafrost peatlands under freeze-thaw cycles.
421 No quantitative relationship was established between both DOC quantity and quality and the
422 number of FTC in the acidic, DOC-rich aqueous leachates of terrestrial vegetation and various
423 peat horizons. We also observed sizable stability of DOC and metal complexes present in
424 typical surface and soil waters of permafrost peatlands with respect to freeze-thaw cycles. The
425 exceptions are the circumneutral, humic- and fulvic-rich waters of the thermokarst lake and
426 the Pechora River, which likely exhibited formation of Fe- and Al-rich organo-mineral particles.
427 In contrast to DOC concentration which remained rather stable with FTC, trace element
428 variations were pronounced and often exceeded 10%. Thus, in the Pechora River water,
429 concentrations of metal micronutrients and trace elements sizably decreased during FTC. This
430 was also partially pronounced in the thermokarst lake water. As such, large water bodies are
431 most subjected by the FTC impact on OM-mineral colloids transport from lakes and rivers to
432 the Arctic Ocean. This impact can be further accentuated due to enhanced FTC frequency
433 under on-going climate warming in high latitudes.

434

435 **Acknowledgements**

436 Supports of RFBR N°19-55-15002, 20-05-00729 and of State Task AAAA-A18-
437 118012390200-5. D.P-R was supported by a PhD. fellowship from the French « Ministère de
438 l'Enseignement Supérieur, de la Recherche et de l'Innovation ». We are grateful to Carole
439 Causserand (GET) for help with DIC and DOC concentrations analyses and to the ICP-MS team
440 of the GET laboratory for the help with the trace elements analyses.

441

442

Conflicts of interest

443

The authors declare no conflict of interest.

References

- 446 Abbt-Braun, G., Frimmel, F.H., 1999. Basic characterization of Norwegian NOM samples — Similarities
447 and differences. *Environ. Int.*, *Nom-typing* 25, 161–180. [https://doi.org/10.1016/S0160-](https://doi.org/10.1016/S0160-4120(98)00118-4)
448 [4120\(98\)00118-4](https://doi.org/10.1016/S0160-4120(98)00118-4)
- 449 Ågren, A., Buffam, I., Berggren, M., Bishop, K., Jansson, M., Laudon, H., 2008. Dissolved organic carbon
450 characteristics in boreal streams in a forest-wetland gradient during the transition between
451 winter and summer. *J. Geophys. Res. Biogeosciences* 113.
452 <https://doi.org/10.1029/2007JG000674>
- 453 Baalousha, M., V. D. Kammer, F., Motelica-Heino, M., Baborowski, M., Hofmeister, C., Le Coustumer,
454 P., 2006. Size-based speciation of natural colloidal particles by flow field flow fractionation,
455 inductively coupled plasma-mass spectroscopy, and transmission electron microscopy/x-ray
456 energy dispersive spectroscopy: colloids–trace element interaction. *Environ. Sci. Technol.* 40,
457 2156–2162. <https://doi.org/10.1021/es051498d>
- 458 Bochove, E. van, Prévost, D., Pelletier, F., 2000. Effects of freeze–thaw and soil structure on nitrous
459 oxide produced in a clay soil. *Soil Sci. Soc. Am. J.* 64, 1638–1643.
460 <https://doi.org/10.2136/sssaj2000.6451638x>
- 461 Boddy, E., Roberts, P., Hill, P.W., Farrar, J., Jones, D.L., 2008. Turnover of low molecular weight
462 dissolved organic C (DOC) and microbial C exhibit different temperature sensitivities in Arctic
463 tundra soils. *Soil Biol. Biochem.* 40, 1557–1566. <https://doi.org/10.1016/j.soilbio.2008.01.030>
- 464 Chapin, F.S., Woodwell, G.M., Randerson, J.T., Rastetter, E.B., Lovett, G.M., Baldocchi, D.D., Clark, D.A.,
465 Harmon, M.E., Schimel, D.S., Valentini, R., Wirth, C., Aber, J.D., Cole, J.J., Goulden, M.L.,
466 Harden, J.W., Heimann, M., Howarth, R.W., Matson, P.A., McGuire, A.D., Melillo, J.M.,
467 Mooney, H.A., Neff, J.C., Houghton, R.A., Pace, M.L., Ryan, M.G., Running, S.W., Sala, O.E.,
468 Schlesinger, W.H., Schulze, E.-D., 2006. reconciling carbon-cycle concepts, terminology, and
469 methods. *ecosystems* 9, 1041–1050. <https://doi.org/10.1007/s10021-005-0105-7>
- 470 Chen, J., Xue, S., Lin, Y., Wang, C., Wang, Q., Han, Q., 2016. Effect of freezing–thawing on dissolved
471 organic matter in water. *Desalination Water Treat.* 57, 17230–17240.
472 <https://doi.org/10.1080/19443994.2015.1085913>
- 473 Chin, Y.-Ping., Aiken, George., O'Loughlin, Edward., 1994. Molecular weight, polydispersity, and
474 spectroscopic properties of aquatic humic substances. *Environ. Sci. Technol.* 28, 1853–1858.
475 <https://doi.org/10.1021/es00060a015>
- 476 Climate & Weather Averages in Naryan-Mar, Russia [WWW Document], 2015. URL
477 <https://www.timeanddate.com/weather/russia/naryan-mar/climate> (accessed 2.24.21).
- 478 Cole, J.J., Prairie, Y.T., Caraco, N.F., McDowell, W.H., Tranvik, L.J., Striegl, R.G., Duarte, C.M.,
479 Kortelainen, P., Downing, J.A., Middelburg, J.J., Melack, J., 2007. Plumbing the global carbon
480 cycle: integrating inland waters into the terrestrial carbon budget. *Ecosystems* 10, 172–185.
481 <https://doi.org/10.1007/s10021-006-9013-8>
- 482 Cory, R.M., Ward, C.P., Crump, B.C., Kling, G.W., 2014. Sunlight controls water column processing of
483 carbon in arctic fresh waters. *Science* 345, 925–928. <https://doi.org/10.1126/science.1253119>
- 484 DeLuca, T.H., Keeney, D.R., McCarty, G.W., 1992. Effect of freeze-thaw events on mineralization of soil
485 nitrogen. *Biol. Fertil. Soils* 14, 116–120. <https://doi.org/10.1007/BF00336260>
- 486 Dillon, P.J., Molot, L.A., 1997. Effect of landscape form on export of dissolved organic carbon, iron, and
487 phosphorus from forested stream catchments. *Water Resour. Res.* 33, 2591–2600.
488 <https://doi.org/10.1029/97WR01921>

489 Elliott, A.C., Henry, H.A.L., 2009. Freeze–thaw cycle amplitude and freezing rate effects on extractable
490 nitrogen in a temperate old field soil. *Biol. Fertil. Soils* 45, 469–476.
491 <https://doi.org/10.1007/s00374-009-0356-0>

492 Fellman, J.B., D’Amore, D.V., Hood, E., 2008. An evaluation of freezing as a preservation technique for
493 analyzing dissolved organic C, N and P in surface water samples. *Sci. Total Environ.* 392, 305–
494 312. <https://doi.org/10.1016/j.scitotenv.2007.11.027>

495 Francko, D.A., 1986. Epilimnetic phosphorus cycling: influence of humic materials and iron on
496 coexisting major mechanisms. *Can. J. Fish. Aquat. Sci.* 43, 302–310.
497 <https://doi.org/10.1139/f86-039>

498 Garcia-Mina, J.M., 2006. Stability, solubility and maximum metal binding capacity in metal–humic
499 complexes involving humic substances extracted from peat and organic compost. *Org.*
500 *Geochem., Advances in Organic Geochemistry 2005* 37, 1960–1972.
501 <https://doi.org/10.1016/j.orggeochem.2006.07.027>

502 Giesy, J.P., Briese, L.A., 1978. Particulate formation due to freezing humic waters. *Water Resour. Res.*
503 14, 542–544. <https://doi.org/10.1029/WR014i003p00542>

504 Guénet, H., Davranche, M., Vantelon, D., Pédrot, M., Al-Sid-Cheikh, M., Dia, A., Jestin, J., 2016.
505 Evidence of organic matter control on As oxidation by iron oxides in riparian wetlands. *Chem.*
506 *Geol.* 439, 161–172. <https://doi.org/10.1016/j.chemgeo.2016.06.023>

507 Henry, H.A.L., 2008. Climate change and soil freezing dynamics: historical trends and projected
508 changes. *Clim. Change* 87, 421–434. <https://doi.org/10.1007/s10584-007-9322-8>

509 Hentschel, K., Borken, W., Matzner, E., 2008. Repeated freeze–thaw events affect leaching losses of
510 nitrogen and dissolved organic matter in a forest soil. *J. Plant Nutr. Soil Sci.* 171, 699–706.
511 <https://doi.org/10.1002/jpln.200700154>

512 Hugelius, G., Strauss, J. (orcid:0000000346784982), Zubrzycki, S. (orcid:0000000263989173), Harden,
513 J.W., Schuur, E. a. G., Ping, C.-L., Schirrmeister, L., Grosse, G., Michaelson, G.J., Koven, C.D.,
514 O’Donnell, J.A., Elberling, B., Mishra, U., Camill, P., Yu, Z., Palmtag, J., Kuhry, P., 2014. Estimated
515 stocks of circumpolar permafrost carbon with quantified uncertainty ranges and identified
516 data gaps. *Biogeosciences Online* 11. <https://doi.org/10.5194/bg-11-6573-2014>

517 Hutchins, R.H.S., Aukes, P., Schiff, S.L., Dittmar, T., Prairie, Y.T., Giorgio, P.A. del, 2017. The optical,
518 chemical, and molecular dissolved organic matter succession along a boreal soil–stream–river
519 continuum. *J. Geophys. Res. Biogeosciences* 122, 2892–2908.
520 <https://doi.org/10.1002/2017JG004094>

521 Iliina, S.M., Lapitskiy, S.A., Alekhin, Y.V., Viers, J., Benedetti, M., Pokrovsky, O.S., 2016. Speciation, Size
522 Fractionation and Transport of Trace Elements in the Continuum Soil Water–Mire–Humic
523 Lake–River–Large Oligotrophic Lake of a Subarctic Watershed. *Aquat. Geochem.* 22, 65–95.
524 <https://doi.org/10.1007/s10498-015-9277-8>

525 Ivarson, K.C., Sowden, F.J., 1970. Effect of frost action and storage of soil at freezing temperatures on
526 the free amino acids, free sugars and respiratory activity of soil. *Can. J. Soil Sci.* 50, 191–198.
527 <https://doi.org/10.4141/cjss70-027>

528 Jones, R.I., Salonen, K., Haan, H.D., 1988. Phosphorus transformations in the epilimnion of humic lakes:
529 abiotic interactions between dissolved humic materials and phosphate. *Freshw. Biol.* 19, 357–
530 369. <https://doi.org/10.1111/j.1365-2427.1988.tb00357.x>

531 Kim, E.-A., Lee, H.K., Choi, J.H., 2017. Effects of a controlled freeze–thaw event on dissolved and
532 colloidal soil organic matter. *Environ. Sci. Pollut. Res.* 24, 1338–1346.
533 <https://doi.org/10.1007/s11356-016-7552-x>

534 Krachler, R., Kammer, F. von der, Jirsa, F., Süphandag, A., Krachler, R.F., Plessl, C., Vogt, M., Keppler,
535 B.K., Hofmann, T., 2012. Nanoscale lignin particles as sources of dissolved iron to the ocean.
536 *Glob. Biogeochem. Cycles* 26. <https://doi.org/10.1029/2012GB004294>

537 Larsen, K.S., Jonasson, S., Michelsen, A., 2002. Repeated freeze–thaw cycles and their effects on
538 biological processes in two arctic ecosystem types. *Appl. Soil Ecol.* 21, 187–195.
539 [https://doi.org/10.1016/S0929-1393\(02\)00093-8](https://doi.org/10.1016/S0929-1393(02)00093-8)

540 Lim, A.G., Loiko, S.V., Kuzmina, D.M., Krickov, I.V., Shirokova, L.S., Kulizhsky, S.P., Vorobyev, S.N.,
541 Pokrovsky, O.S., 2021. Dispersed ground ice of permafrost peatlands: Potential unaccounted
542 carbon, nutrient and metal sources. *Chemosphere* 266, 128953.
543 <https://doi.org/10.1016/j.chemosphere.2020.128953>

544 Lipson, D.A., Monson, R.K., 1998. Plant-microbe competition for soil amino acids in the alpine tundra:
545 effects of freeze-thaw and dry-rewet events. *Oecologia* 113, 406–414.
546 <https://doi.org/10.1007/s004420050393>

547 Ma, Q., Jin, H., Yu, C., Bense, V.F., 2019. Dissolved organic carbon in permafrost regions: A review. *Sci.*
548 *China Earth Sci.* 62, 349–364. <https://doi.org/10.1007/s11430-018-9309-6>

549 Malcolm, R.L., 1990. The uniqueness of humic substances in each of soil, stream and marine
550 environments. *Anal. Chim. Acta* 232, 19–30.

551 Malmer, N., Johansson, T., Olsrud, M., Christensen, T.R., 2005. Vegetation, climatic changes and net
552 carbon sequestration in a North-Scandinavian subarctic mire over 30 years. *Glob. Change Biol.*
553 11, 1895–1909. <https://doi.org/10.1111/j.1365-2486.2005.01042.x>

554 Manasypov, R.M., Vorobyev, S.N., Loiko, S.V., Kritzkov, I.V., Shirokova, L.S., Shevchenko, V.P., Kirpotin,
555 S.N., Kulizhsky, S.P., Kolesnichenko, L.G., Zemtsov, V.A., Sinkinov, V.V., Pokrovsky, O.S., 2015.
556 Seasonal dynamics of organic carbon and metals in thermokarst lakes from the discontinuous
557 permafrost zone of western Siberia. *Biogeosciences* 12, 3009–3028.
558 <https://doi.org/10.5194/bg-12-3009-2015>

559 McGuire, A.D., Lawrence, D.M., Koven, C., Klein, J.S., Burke, E., Chen, G., Jafarov, E., MacDougall, A.H.,
560 Marchenko, S., Nicolsky, D., Peng, S., Rinke, A., Ciais, P., Gouttevin, I., Hayes, D.J., Ji, D., Krinner,
561 G., Moore, J.C., Romanovsky, V., Schädel, C., Schaefer, K., Schuur, E.A.G., Zhuang, Q., 2018.
562 Dependence of the evolution of carbon dynamics in the northern permafrost region on the
563 trajectory of climate change. *Proc. Natl. Acad. Sci.* 115, 3882–3887.
564 <https://doi.org/10.1073/pnas.1719903115>

565 Morgalev, Y.N., Lushchaeva, I.V., Morgaleva, T.G., Kolesnichenko, L.G., Loiko, S.V., Krickov, I.V., Lim, A.,
566 Raudina, T.V., Volkova, I.I., Shirokova, L.S., Morgalev, S.Y., Vorobyev, S.N., Kirpotin, S.N.,
567 Pokrovsky, O.S., 2017. Bacteria primarily metabolize at the active layer/permafrost border in
568 the peat core from a permafrost region in western Siberia. *Polar Biol.* 40, 1645–1659.
569 <https://doi.org/10.1007/s00300-017-2088-1>

570 Oleinikova, O.V., Shirokova, L.S., Drozdova, O.Y., Lapitskiy, S.A., Pokrovsky, O.S., 2018. Low
571 biodegradability of dissolved organic matter and trace metals from subarctic waters. *Science*
572 *of The Total Environment* 618, 174–187. <https://doi.org/10.1016/j.scitotenv.2017.10.340>

573 Oleinikova, O.V., Shirokova, L.S., Gérard, E., Drozdova, O.Yu., Lapitskiy, S.A., Bychkov, A.Yu., Pokrovsky,
574 O.S., 2017. Transformation of organo-ferric peat colloids by a heterotrophic bacterium.
575 *Geochimica et Cosmochimica Acta* 205, 313–330. <https://doi.org/10.1016/j.gca.2017.02.029>

576 Park, S., Joe, K.S., Han, S.H., Kim, H.S., 1999. characteristics of dissolved organic carbon in the leachate
577 from Moonam Sanitary Landfill. *Environ. Technol.* 20, 419–424.
578 <https://doi.org/10.1080/09593332008616835>

579 Payandi-Rolland, D., Shirokova, L.S., Labonne, F., Bénézech, P., Pokrovsky, O.S., 2020a. Data from Low
580 impact of FTC on organic carbon and metals in waters of permafrost peatlands, Mendeley
581 Data, V1. <http://dx.doi.org/10.17632/656f9skxp4.1>

582 Payandi-Rolland, D., Shirokova, L.S., Nakhle, P., Tesfa, M., Abdou, A., Causserand, C., Lartiges, B., Rols,
583 J.-L., Guérin, F., Bénézech, P., Pokrovsky, O.S., 2020b. Aerobic release and biodegradation of

584 dissolved organic matter from frozen peat: Effects of temperature and heterotrophic bacteria.
585 Chem. Geol. 536, 119448. <https://doi.org/10.1016/j.chemgeo.2019.119448>

586 Petzold, G., Niranjana, K., Aguilera, J.M., 2013. Vacuum-assisted freeze concentration of sucrose
587 solutions. J. Food Eng. 115, 357–361. <https://doi.org/10.1016/j.jfoodeng.2012.10.048>

588 Pokrovsky, O.S., Karlsson, J., Giesler, R., 2018. Freeze-thaw cycles of Arctic thaw ponds remove colloidal
589 metals and generate low-molecular-weight organic matter. Biogeochemistry 137, 321–336.
590 <https://doi.org/10.1007/s10533-018-0421-6>

591 Pokrovsky, O.S., Manasypov, R.M., Kopysov, S.G., Krickov, I.V., Shirokova, L.S., Loiko, S.V., Lim, A.G.,
592 Kolesnichenko, L.G., Vorobyev, S.N., Kirpotin, S.N., 2020. Impact of permafrost thaw and
593 climate warming on riverine export fluxes of carbon, nutrients and metals in western Siberia.
594 Water 12, 1817. <https://doi.org/10.3390/w12061817>

595 Pokrovsky, O.S., Manasypov, R.M., Loiko, S.V., Shirokova, L.S., 2016. Organic and organo-mineral
596 colloids in discontinuous permafrost zone. Geochim. Cosmochim. Acta 188, 1–20.
597 <https://doi.org/10.1016/j.gca.2016.05.035>

598 Poulin, B.A., Ryan, J.N., Aiken, G.R., 2014. Effects of iron on optical properties of dissolved organic
599 matter. Environ. Sci. Technol. 48, 10098–10106. <https://doi.org/10.1021/es502670r>

600 Ren, J., Vanapalli, S.K., 2020. Effect of freeze–thaw cycling on the soil-freezing characteristic curve of
601 five Canadian soils. Vadose Zone J. 19, e20039. <https://doi.org/10.1002/vzj2.20039>

602 Romanovsky, V.E., Smith, S.L., Christiansen, H.H., 2010. Permafrost thermal state in the polar Northern
603 Hemisphere during the international polar year 2007–2009: a synthesis. Permafr. Periglac.
604 Process. 21, 106–116. <https://doi.org/10.1002/ppp.689>

605 Savenko, A.V., Savenko, V.S., Pokrovsky, O.S., 2020. Phase fractionation of chemical elements during
606 the formation of ice in fresh surface waters. Dokl. Earth Sci. 492, 327–332.
607 <https://doi.org/10.1134/S1028334X20050207>

608 Schimel, J.P., Clein, J.S., 1996. Microbial response to freeze-thaw cycles in tundra and taiga soils. Soil
609 Biol. Biochem. 28, 1061–1066. [https://doi.org/10.1016/0038-0717\(96\)00083-1](https://doi.org/10.1016/0038-0717(96)00083-1)

610 Schuur, E.A.G., McGuire, A.D., Schädel, C., Grosse, G., Harden, J.W., Hayes, D.J., Hugelius, G., Koven,
611 C.D., Kuhry, P., Lawrence, D.M., Natali, S.M., Olefeldt, D., Romanovsky, V.E., Schaefer, K.,
612 Turetsky, M.R., Treat, C.C., Vonk, J.E., 2015. Climate change and the permafrost carbon
613 feedback. Nature 520, 171–179. <https://doi.org/10.1038/nature14338>

614 Selvam, B.P., Lapierre, J.-F., Soares, A.R.A., Bastviken, D., Karlsson, J., Berggren, M., 2019. Photo-
615 reactivity of dissolved organic carbon in the freshwater continuum. Aquat. Sci. 81, 57.
616 <https://doi.org/10.1007/s00027-019-0653-0>

617 Serikova, S., Pokrovsky, O.S., Laudon, H., Krickov, I.V., Lim, A.G., Manasypov, R.M., Karlsson, J., 2019.
618 High carbon emissions from thermokarst lakes of Western Siberia. Nature Communications 10,
619 1552. <https://doi.org/10.1038/s41467-019-09592-1>

620 Shafique, U., Anwar, J., uz-Zaman, W., Rehman, R., Salman, M., Dar, A., Jamil, N., 2012. Forced
621 migration of soluble and suspended materials by freezing front in aqueous systems. J. Hydro-
622 Environ. Res. 6, 221–226. <https://doi.org/10.1016/j.jher.2011.10.001>

623 Shirokova, L.S., Chupakov, A.V., Zabelina, S.A., Neverova, N.V., Payandi-Rolland, D., Causserand, C.,
624 Karlsson, J., Pokrovsky, O.S., 2019. Humic surface waters of frozen peat bogs (permafrost zone)
625 are highly resistant to bio- and photodegradation. Biogeosciences 16, 2511–2526.
626 <https://doi.org/10.5194/bg-16-2511-2019>

627 Shirokova, L., Ivanova, I., Manasypov, R., Pokrovsky, O., Chupakov, A., Iglovsky, S., Shorina, N., Zabelina,
628 S., Gofarov, M., Payandi-Rolland, D., Chupakova, A., Moreva, O., 2019. The evolution of the
629 ecosystems of thermokarst lakes of the Bolshezemel'skaya tundra in the context of climate
630 change. E3S Web Conf. 98, 02010. <https://doi.org/10.1051/e3sconf/20199802010>

631 Shirokova, L.S., Bredoire, R., Rols, J.-L., Pokrovsky, O.S., 2017a. Moss and peat leachate degradability
632 by heterotrophic bacteria: the fate of organic carbon and trace metals. *Geomicrobiol. J.* 34,
633 641–655. <https://doi.org/10.1080/01490451.2015.1111470>

634 Shirokova, L.S., Labouret, J., Gurge, M., Gérard, E., Ivanova, I.S., Zabelina, S.A., Pokrovsky, O.S., 2017b.
635 Impact of cyanobacterial associate and heterotrophic bacteria on dissolved organic carbon and
636 metal in moss and peat leachate: application to permafrost thaw in aquatic environments.
637 *Aquat. Geochem.* 23, 331–358. <https://doi.org/10.1007/s10498-017-9325-7>

638 Spencer, R.G.M., Bolton, L., Baker, A., 2007. Freeze/thaw and pH effects on freshwater dissolved
639 organic matter fluorescence and absorbance properties from a number of UK locations. *Water*
640 *Res.* 41, 2941–2950. <https://doi.org/10.1016/j.watres.2007.04.012>

641 Stolpe, B., Guo, L., Shiller, A.M., Aiken, G.R., 2013. Abundance, size distributions and trace-element
642 binding of organic and iron-rich nanocolloids in Alaskan rivers, as revealed by field-flow
643 fractionation and ICP-MS. *Geochim. Cosmochim. Acta* 105, 221–239.
644 <https://doi.org/10.1016/j.gca.2012.11.018>

645 Stres, B., Philippot, L., Faganeli, J., Tiedje, J.M., 2010. Frequent freeze–thaw cycles yield diminished yet
646 resistant and responsive microbial communities in two temperate soils: a laboratory
647 experiment. *FEMS Microbiol. Ecol.* 74, 323–335. [https://doi.org/10.1111/j.1574-](https://doi.org/10.1111/j.1574-6941.2010.00951.x)
648 [6941.2010.00951.x](https://doi.org/10.1111/j.1574-6941.2010.00951.x)

649 Tierney, G.L., Fahey, T.J., Groffman, P.M., Hardy, J.P., Fitzhugh, R.D., Driscoll, C.T., 2001. Soil freezing
650 alters fine root dynamics in a northern hardwood forest. *Biogeochemistry* 56, 175–190.
651 <https://doi.org/10.1023/A:1013072519889>

652 Tranvik, L.J., Jørgensen, N.O., 1995. Colloidal and dissolved organic matter in lake water: carbohydrate
653 and amino acid composition, and ability to support bacterial growth. *Biogeochemistry* 30, 77–
654 97.

655 Tukey, J.W., 1977. *Exploratory data analysis*. Reading, Mass.

656 Vestgarden, L.S., Austnes, K., 2009. Effects of freeze–thaw on C and N release from soils below different
657 vegetation in a montane system: a laboratory experiment. *Glob. Change Biol.* 15, 876–887.
658 <https://doi.org/10.1111/j.1365-2486.2008.01722.x>

659 Vonk, J.E., Tank, S.E., Bowden, W.B., Laurion, I., Vincent, W.F., Alekseychik, P., Amyot, M., Billet, M.F.,
660 Canario, J., Cory, R.M., Deshpande, B.N., Helbig, M., Jammet, M., Karlsson, J., Larouche, J.,
661 MacMillan, G., Rautio, M., Anthony, K.M.W., Wickland, K.P., 2015. Reviews and syntheses:
662 Effects of permafrost thaw on Arctic aquatic ecosystems. *Biogeosciences* 12, 7129–7167.

663 Weishaar, J.L., Aiken, G.R., Bergamaschi, B.A., Fram, M.S., Fujii, R., Mopper, K., 2003. evaluation of
664 specific ultraviolet absorbance as an indicator of the chemical composition and reactivity of
665 dissolved organic carbon. *Environ. Sci. Technol.* 37, 4702–4708.
666 <https://doi.org/10.1021/es030360x>

667 Xiao, L., Zhang, Yang, Li, P., Xu, G., Shi, P., Zhang, Yi, 2019. Effects of freeze-thaw cycles on aggregate-
668 associated organic carbon and glomalin-related soil protein in natural-succession grassland
669 and Chinese pine forest on the Loess Plateau. *Geoderma* 334, 1–8.
670 <https://doi.org/10.1016/j.geoderma.2018.07.043>

671 Xue, S., Wen, Y., Hui, X., Zhang, L., Zhang, Z., Wang, J., Zhang, Y., 2015. The migration and
672 transformation of dissolved organic matter during the freezing processes of water. *J. Environ.*
673 *Sci.* 27, 168–178. <https://doi.org/10.1016/j.jes.2014.05.035>

674 Young, K.C., Docherty, K.M., Maurice, P.A., Bridgham, S.D., 2005. Degradation of surface-water
675 dissolved organic matter: influences of DOM chemical characteristics and microbial
676 populations. *Hydrobiologia* 539, 1–11. <https://doi.org/10.1007/s10750-004-3079-0>

677 Yu, X., Zou, Y., Jiang, M., Lu, X., Wang, G., 2011. Response of soil constituents to freeze–thaw cycles in
678 wetland soil solution. *Soil Biol. Biochem.* 43, 1308–1320.
679 <https://doi.org/10.1016/j.soilbio.2011.03.002>
680 Zaritzky, N., 2006. Physical-chemical principles in freezing. *Food Sci. Technol.*-N. Y.-Marcel Dekker- 155,
681 3.

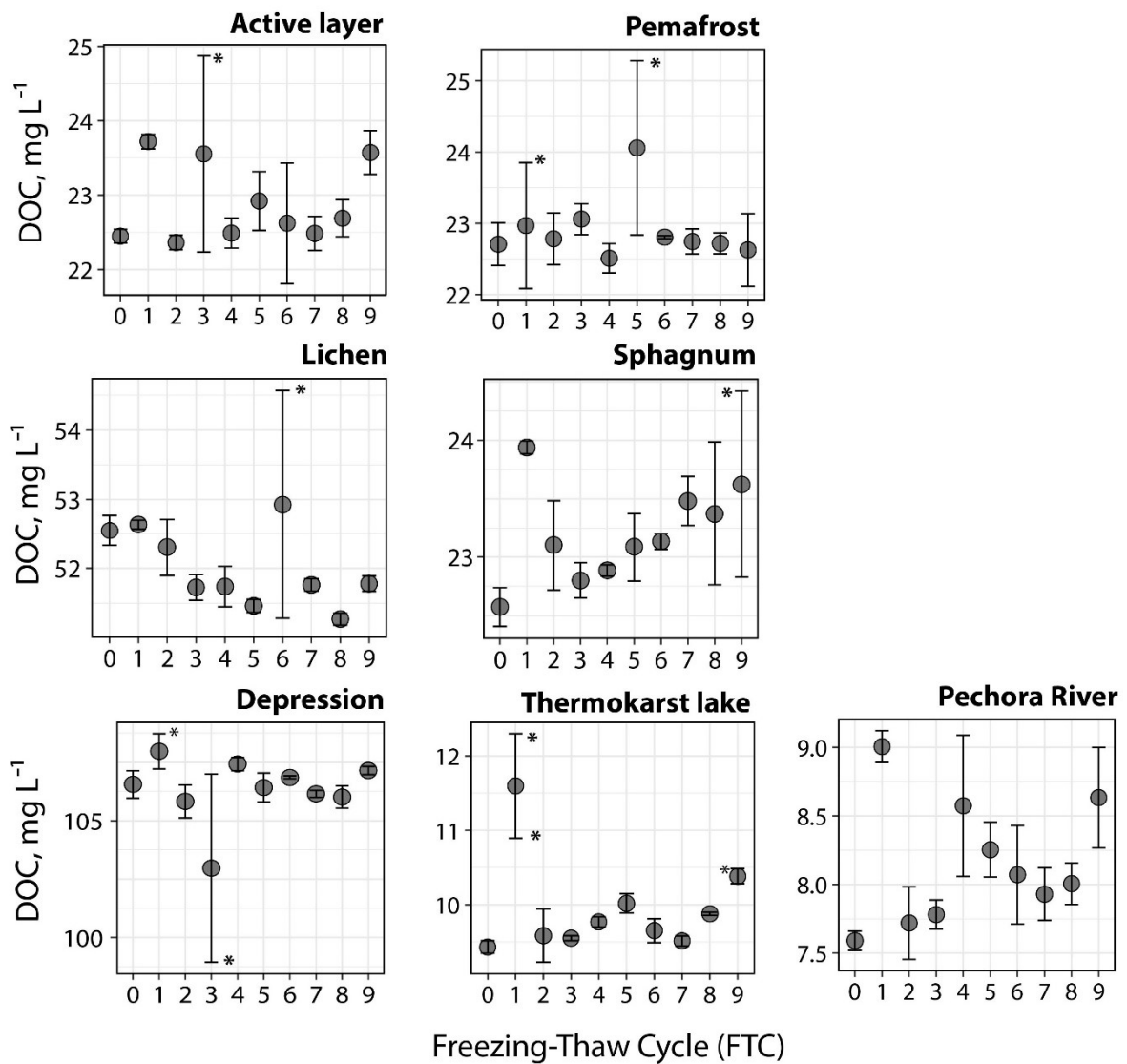
682 **Tables and Figures**

683 *Tables*

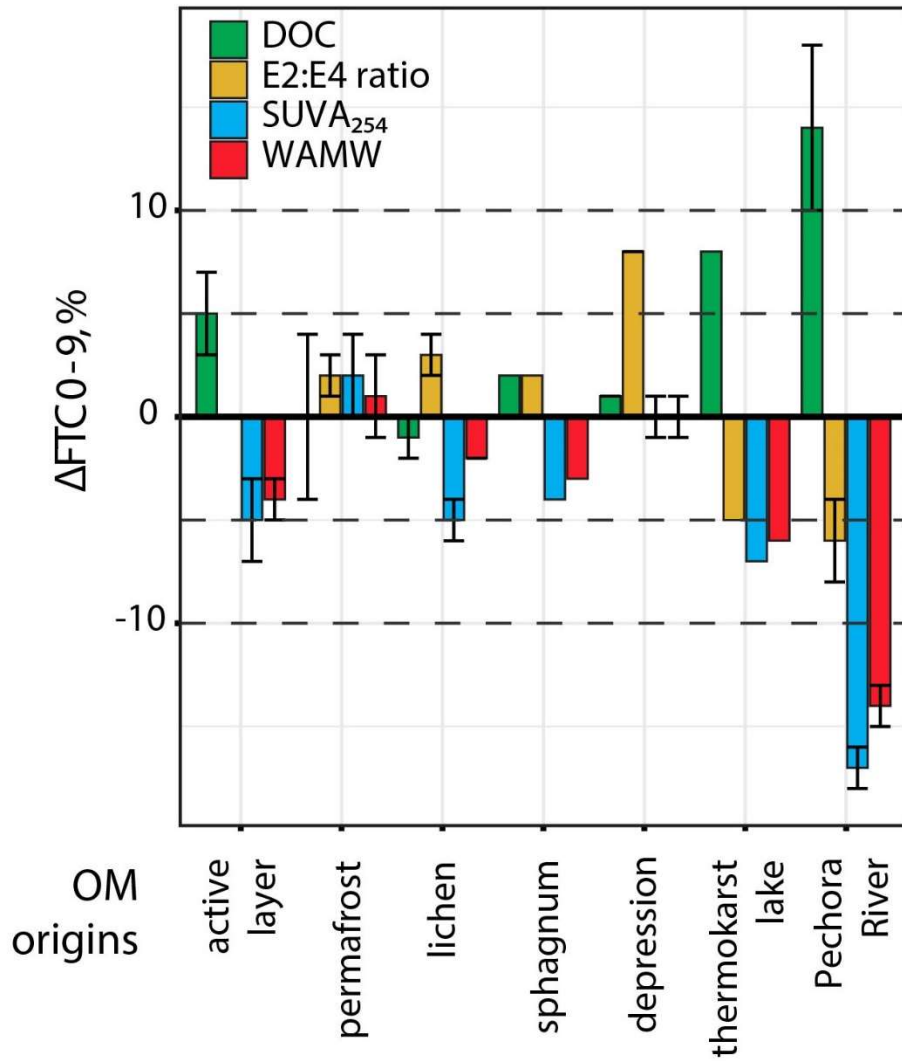
684 **Table 1:** General physical and chemical dissolved (<0.22 µm) parameters of different aquatic substrates before the first freezing (replicate
685 mean).

	Abbreviation, units	Leachates				Natural waters		
		Frozen peat		Vegetation		depression	thermokarst lake	Pechora River
		active layer	permafrost	lichen	moss			
Acidity	pH, E	4.3	4.6	4.6	5.5	6.4	6.3	7.0
	Conductivity, µS cm ⁻¹	21.0	17.0	28.0	25.0	141	18.0	77.0
Carbon	DOC, mg L ⁻¹	22.5	22.7	52.6	22.6	106	9.40	7.60
	DIC, mg L ⁻¹	0.63	0.63	0.66	0.89	0.80	1.40	10.4
	SUVA ₂₅₄ , L mgC ⁻¹ m ⁻¹	5.3	5.2	0.7	5.2	1.6	4.5	4.0
	E2:E3 ratio	3.50	3.50	3.80	3.90	4.70	3.70	3.50
	E2:E4 ratio	13.4	13.5	11.3	13.5	17.9	10.6	9.50
	E4:E6 ratio	7.00	7.20	3.60	5.50	5.20	4.60	4.00
	WAMW, Da	2525	2489	758	2429	1121	2167	1999
Alkali metals	Na, µg L ⁻¹	106	156	701	1171	6787	682	1955
	K, µg L ⁻¹	48.9	54.2	2658	223	1483	159	196
	Rb, µg L ⁻¹	0.20	0.27	5.08	0.13	28.3	0.19	0.21
Alkaline-earth metals	Mg, µg L ⁻¹	50.2	65.8	8.12	440	128	342	1521
	Ca, µg L ⁻¹	295.6	419	29.9	922	163	887	7097
	Sr, µg L ⁻¹	1.37	1.87	0.08	5.59	0.74	3.69	32.2
	Ba, µg L ⁻¹	0.36	0.37	0.13	2.70	0.46	2.06	3.37

Micro- and Macro- nutrients	Si, $\mu\text{g L}^{-1}$	67.7	64.5	147	1730	271	30.3	1302
	P, $\mu\text{g L}^{-1}$	6.20	6.91	11.0	703	286	706	652
	Cr, $\mu\text{g L}^{-1}$	0.14	0.23	0.30	0.53	0.30	0.08	0.07
	V, $\mu\text{g L}^{-1}$	0.63	0.89	0.03	0.14	0.63	0.10	0.15
	Mn, $\mu\text{g L}^{-1}$	5.82	8.79	0.70	11.1	5.72	0.35	0.78
	Fe, $\mu\text{g L}^{-1}$	81.3	123	4.76	476	1327	66.9	180
	Co, $\mu\text{g L}^{-1}$	0.17	0.23	0.02	0.25	1.26	0.01	0.00
	Ni, $\mu\text{g L}^{-1}$	0.53	0.72	0.07	0.92	1.54	0.45	0.44
Mo, $\mu\text{g L}^{-1}$	0.02	0.03	0.02	0.00	0.27	0.01	0.09	
Trivalent hydrolysates	Al, $\mu\text{g L}^{-1}$	23.7	26.8	11.2	207	93.9	25.9	5.43
	Ga, $\mu\text{g L}^{-1}$	0.00	0.01	0.00	0.01	0.04	0.00	0.00
	Y, $\mu\text{g L}^{-1}$	0.01	0.01	0.01	0.20	0.01	0.06	0.07
	La, $\mu\text{g L}^{-1}$	0.01	0.02	0.02	0.20	0.02	0.05	0.06
	Ce, $\mu\text{g L}^{-1}$	0.01	0.01	0.04	0.52	0.03	0.11	0.07
	Pr, $\mu\text{g L}^{-1}$	0.00	0.00	0.00	0.06	0.00	0.01	0.01
	Nd, $\mu\text{g L}^{-1}$	0.01	0.01	0.01	0.25	0.01	0.06	0.07
	Dy, $\mu\text{g L}^{-1}$	0.00	0.00	0.00	0.04	0.00	0.01	0.01
Yb, $\mu\text{g L}^{-1}$	0.00	0.00	0.00	0.02	0.00	0.01	0.01	
Tetravalent hydrolysates	Ti, $\mu\text{g L}^{-1}$	0.06	0.07	0.27	0.75	0.37	0.13	0.16
	Zr, $\mu\text{g L}^{-1}$	0.04	0.05	0.02	0.32	0.09	0.06	0.03
	Hf, $\mu\text{g L}^{-1}$	0.00	0.00	0.00	0.01	0.00	0.00	0.00
	Th, $\mu\text{g L}^{-1}$	0.00	0.00	0.01	0.06	0.00	0.00	0.00
Toxicants	As, $\mu\text{g L}^{-1}$	0.83	1.18	0.07	0.19	0.20	0.36	0.76
	Pb, $\mu\text{g L}^{-1}$	0.03	0.02	0.04	0.20	0.06	0.06	0.69

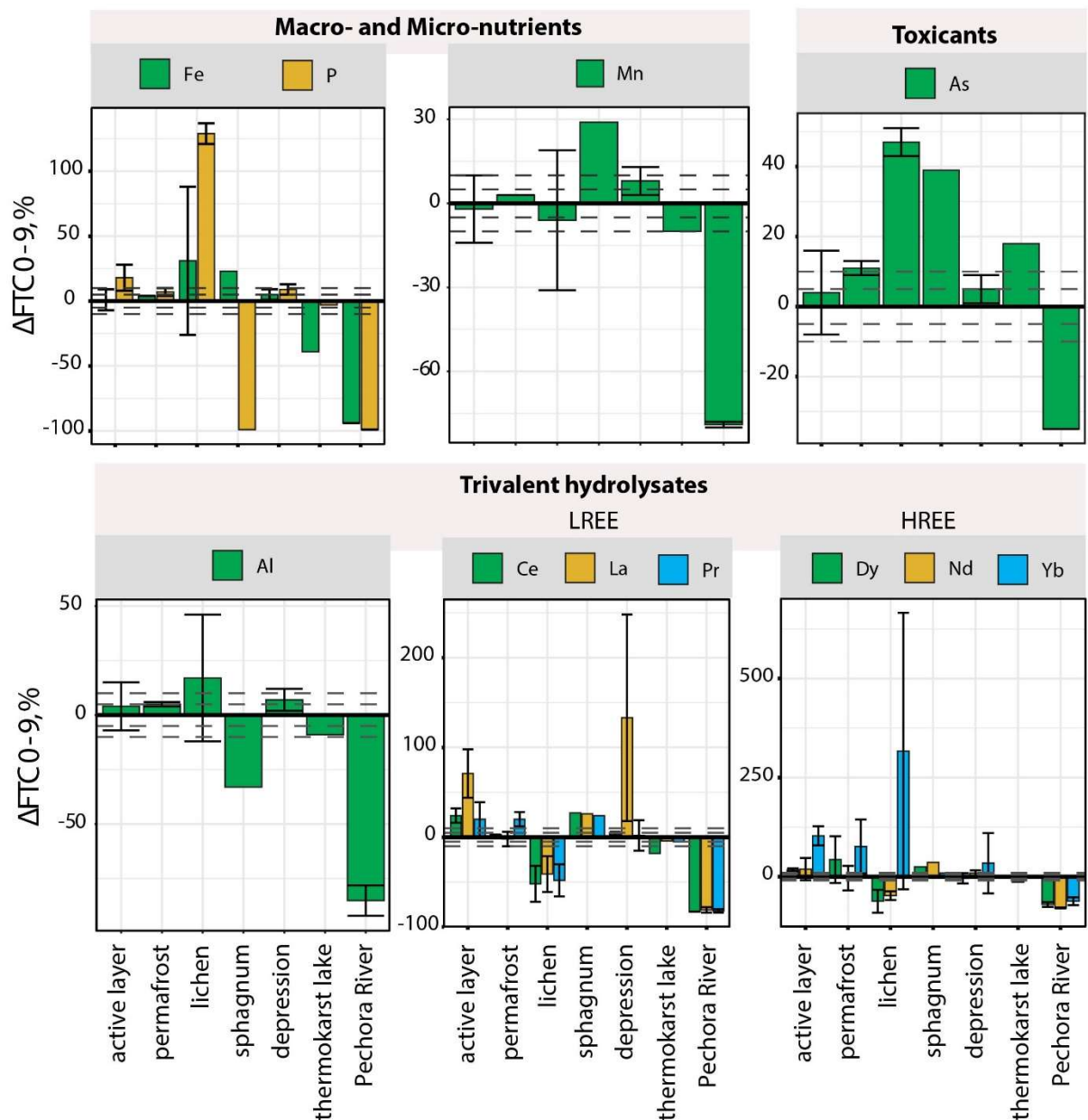


690 **Figure 1:** DOC concentration during FTC for each type of waters incubations. “*” indicates the
 691 replicate for which data is considered as outliers by boxplots analyses.



693

694 **Figure 2:** Percent variation (Δ , %) of DOC quantity and quality parameters (DOC concentration,
 695 SUVA₂₅₄, E2:E4 ratio and Weight-Average Molecular Weight (WAMW)) between final (FTC 9)
 696 and initial (FTC 0) steps of the freezing-thawing experiment. Error bars presented here reflect
 697 the standard deviation of replicates.



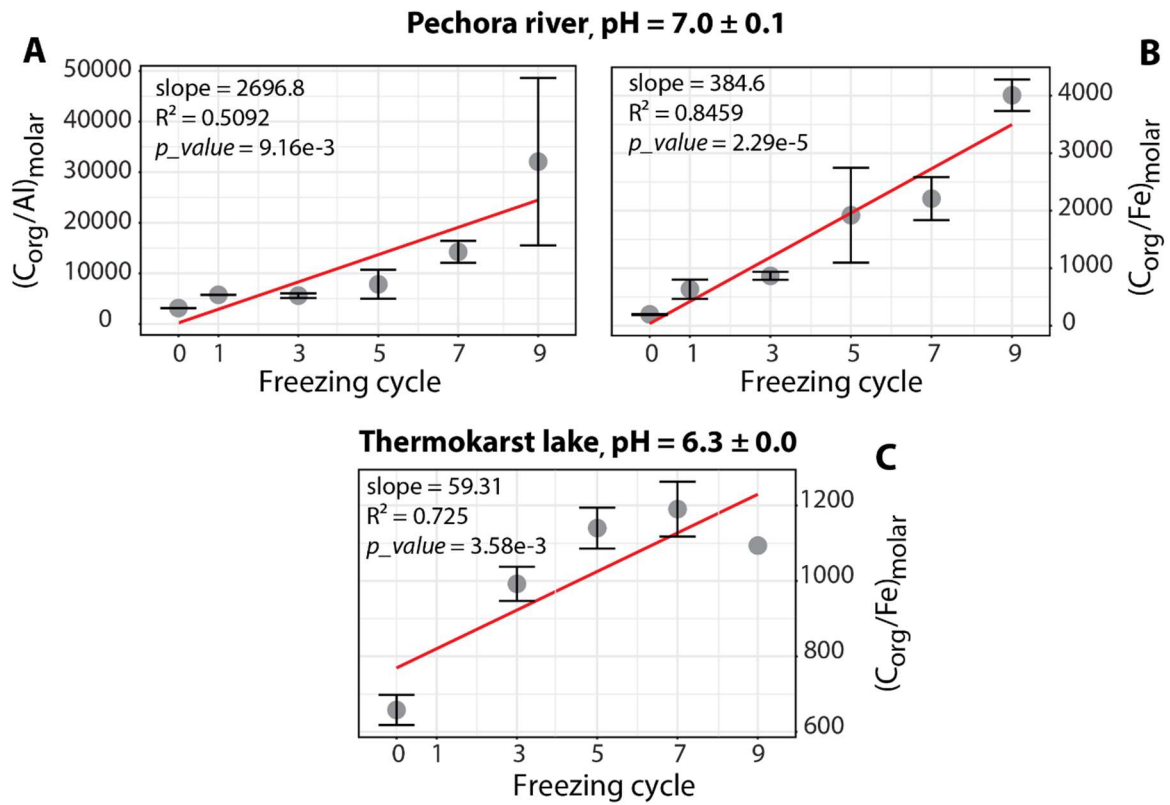
698

699 **Figure 3:** Percent variation of trivalent hydrolysates (Al, Light and Heavy Rare Earth Elements

700 (LREE and HREE)), Macro- and Micro-nutrients (Fe, P, and Mn) and toxicant (As) concentrations

701 between the last and the initial stage of FTC ($\Delta\text{FTCO-9}$). Vertical dashed lines indicate variations

702 of 5 and 10% (under and above 0). Errors bars represent the variation between replicates.



703

704 **Figure 4:** The molar ratio of C_{org} (A) to Al and (B) to Fe for the Pechora River substrate, and the
 705 molar ratio of C_{org} (C) to Fe for the thermokarst lake in the course of FTC. The red lines
 706 represent the linear regression. Error bars represent the variation between replicates.

707